RECENT PROGRESS ON THE DETERMINATION OF THE SYMMETRY ENERGY

LIE-WEN CHEN[1,2]

[1] *INPAC, Department of Physics and Shanghai Key Laboratory for Particle Physics and Cosmology, Shanghai Jiao Tong University, Shanghai 200240, China*
[2] *Center of Theoretical Nuclear Physics, National Laboratory of Heavy-Ion Accelerator, Lanzhou, 730000, China*
E-mail: lwchen@sjtu.edu.cn

We summarize the current status on constraining the density dependence of the symmetry energy from terrestrial laboratory measurements and astrophysical observations. While the value $E_{\mathrm{sym}}(\rho_0)$ and density slope L of the symmetry energy at saturation density ρ_0 can vary largely depending on the data or methods, all the existing constraints are essentially consistent with $E_{\mathrm{sym}}(\rho_0) = 31 \pm 2$ MeV and $L = 50 \pm 20$ MeV. The determination of the supra-saturation density behavior of the symmetry energy remains a big challenge.

Keywords: The symmetry energy; Equation of state for asymmetric nuclear matter; Nuclear reactions; Nuclear structures; Neutron stars.

1. Introduction

In nuclear physics and astrophysics, there is currently of great interest to determine the density dependence of the nuclear symmetry energy $E_{\mathrm{sym}}(\rho)$ that essentially characterizes the isospin dependent part of the equation of state (EOS) of asymmetric nuclear matter. The exact knowledge on the symmetry energy is important for understanding not only many problems in nuclear physics, such as the structure of radioactive nuclei, the reaction dynamics induced by rare isotopes, the liquid-gas phase transition in asymmetric nuclear matter, and the isospin evolution of QCD phase diagram at finite baryon chemical potential, but also many critical issues such as the properties of neutron stars and supernova explosion mechanism in astrophysics.[1–5] The symmetry energy may also be relevant to some interesting issues regarding possible new physics beyond the standard model.[6–8] During the last decade, although significant progress has been made both experimentally and theoretically on constraining the density dependence of the

2

symmetry energy,[3,5] large uncertainties on $E_{\mathrm{sym}}(\rho)$ still exist, especially its super-normal density behavior remains elusive and largely controversial.[9–12] To reduce the uncertainties of the constraints on $E_{\mathrm{sym}}(\rho)$ thus provides a strong motivation for studying isospin nuclear physics in radioactive nuclei at the new/planning rare isotope beam facilities around the world, such as CSR/Lanzhou and BRIF-II/Beijing in China, RIBF/RIKEN in Japan, SPIRAL2/GANIL in France, FAIR/GSI in Germany, FRIB/NSCL in USA, SPES/LNL in Italy, and KoRIA in Korea.

In the present talk, we summarize the current status on constraining the density dependence of the symmetry energy from terrestrial laboratory measurements and astrophysical observations, including nuclear reactions, nuclear structures, and the properties of neutron stars.

2. The symmetry energy

The EOS of isospin asymmetric nuclear matter, given by its binding energy per nucleon, can be expanded to 2nd-order in isospin asymmetry δ as

$$E(\rho, \delta) = E_0(\rho) + E_{\mathrm{sym}}(\rho)\delta^2 + O(\delta^4), \tag{1}$$

where $\rho = \rho_n + \rho_p$ is the baryon density with ρ_n and ρ_p denoting the neutron and proton densities, respectively; $\delta = (\rho_n - \rho_p)/(\rho_p + \rho_n)$ is the isospin asymmetry; $E_0(\rho) = E(\rho, \delta = 0)$ is the binding energy per nucleon in symmetric nuclear matter, and the symmetry energy is expressed as

$$E_{\mathrm{sym}}(\rho) = \frac{1}{2!}\frac{\partial^2 E(\rho, \delta)}{\partial \delta^2}\Big|_{\delta=0}. \tag{2}$$

Neglecting the contribution from higher-order terms in Eq. (1) leads to the well-known empirical parabolic law for the EOS of asymmetric nuclear matter, which has been verified by all many-body theories to date, at least for densities up to moderate values.[5,13] As a good approximation, the density-dependent symmetry energy $E_{\mathrm{sym}}(\rho)$ can thus be extracted from the parabolic approximation as

$$E_{\mathrm{sym}}(\rho) \approx E(\rho, \delta = 1) - E(\rho, \delta = 0). \tag{3}$$

Around the saturation density ρ_0, the nuclear symmetry energy $E_{\mathrm{sym}}(\rho)$ can be expanded, e.g., up to 2nd-order in density, as

$$E_{\mathrm{sym}}(\rho) = E_{\mathrm{sym}}(\rho_0) + L\chi + \frac{K_{\mathrm{sym}}}{2!}\chi^2 + O(\chi^3), \tag{4}$$

where $\chi = \frac{\rho - \rho_0}{3\rho_0}$ is a dimensionless variable characterizing the deviations of the density from ρ_0, and L and K_{sym} are the slope parameter and curvature

parameter, respectively, i.e.,

$$L = 3\rho_0 \frac{dE_{\text{sym}}(\rho)}{\partial \rho}|_{\rho=\rho_0}, K_{\text{sym}} = 9\rho_0^2 \frac{d^2 E_{\text{sym}}(\rho)}{\partial \rho^2}|_{\rho=\rho_0}. \tag{5}$$

3. The symmetry energy around the saturation density

During the last decade, a number of experimental probes have been proposed to constrain the density dependence of the symmetry energy. Most of them are for the symmetry energy around the saturation density while a few of probes are for the supra-saturation density behaviors. In this section, we summarize the present status on constraining the symmetry energy around the saturation density, mainly, the parameters $E_{\text{sym}}(\rho_0)$ and L, from nuclear reactions, nuclear structures, and the properties of neutron stars.

3.1. *Nuclear reactions*

Nuclear reactions, mainly including heavy ion collisions and nucleon-nucleus scattering, provide an important tool to explore the density dependence of the symmetry energy.

3.1.1. *Heavy ion collisions*

One important progress on constraining the density dependence of the symmetry energy is from the isospin dependent Boltzmann-Uehling-Uhlenbeck (IBUU04) transport model analysis[14] on the isospin diffusion data from NSCL-MSU.[15] It is found that the degree of isospin diffusion in heavy-ion collisions is affected by both the stiffness of the nuclear symmetry energy and the momentum dependence of the nucleon potential. Using a momentum dependence derived from the Gogny effective interaction and the corresponding isospin dependent in-medium nucleon-nucleon scattering cross sections, the experimental data from NSCL-MSU on isospin diffusion leads to a constraint of $L = 86 \pm 25$ MeV with $E_{\text{sym}}(\rho_0) = 30.5$ MeV,[14,16] which is shown as a solid square with error bar with a label "**Iso. Diff. (IBUU04,2005)**" in Fig. 1. It should be mentioned that the constraint in the original publication[14,16] is $L = 88 \pm 25$ MeV and $E_{\text{sym}}(\rho_0) = 31.6$ MeV, due to the application of the parabolic approximation Eq. (3) for the symmetry energy. This constraint is significantly softer than the prediction by transport model simulation with momentum-independent interaction[15] and in agreement with microscopic theoretical calculations.

The isoscaling of the fragment yields in heavy ion collisions has been shown to be a good probe of the symmetry energy.[17] By analyzing
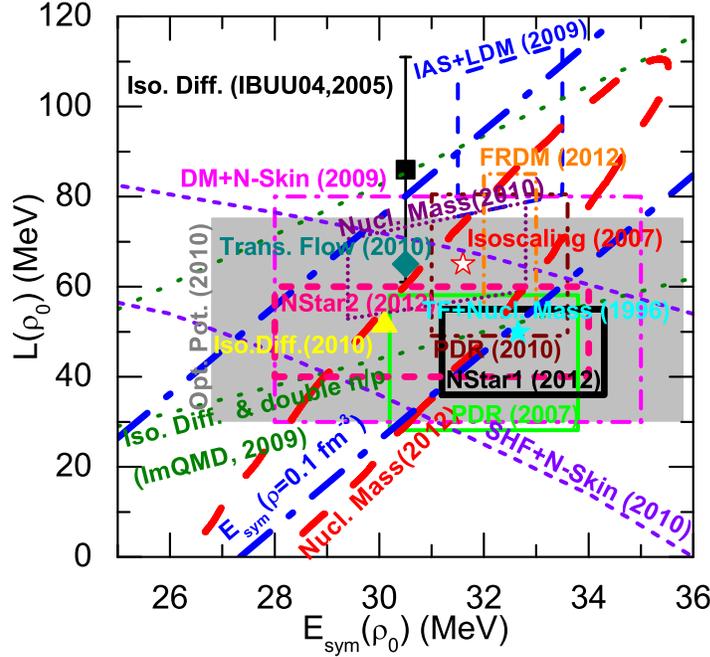
4

Fig. 1.   (Color online) Constraints on $E_{sym}(\rho_0)$ and L from different experiments or methods. See text for details.

the isoscaling of the fragment yields in Ar+Fe/Ca+Ni, Fe+Fe/Ni+Ni, Ar+Ni/Ca+Ni, and Fe+Ni/Ni+Ni reactions at Fermi energy region, within the antisymmetrized molecular dynamic (AMD) model, a constraint of $E_{sym}(\rho_0) = 31.6$ MeV and $L = 65 \pm 25$ MeV has been obtained in Ref.,[18] which is denoted by a open star with a label "**Isoscaling (2007)**" in Fig. 1.

The double ratios of neutron and proton energy spectra in heavy ion collisions provide a good probe of the symmetry energy. An improved quantum molecular dynamics (ImQMD) transport model analysis[19] of the isospin diffusion data from two different observables and the ratios of neutron and proton spectra in collisions at E/A= 50 MeV involving ^{112}Sn and ^{124}Sn nuclei has led to a constraint on $E_{sym}(\rho_0)$ and L at 95% confidence level, corresponding to 2 standard deviations from the minimum χ^2. This constraint is denoted by the region between two dotted lines with a label "**Iso. Diff. & double n/p (ImQMD, 2009)**" in Fig. 1. A more recent ImQMD model analysis[20] of the isospin diffusion data from heavy ion collisions at lower incident energy (E/A= 35 MeV) involving ^{112}Sn and ^{124}Sn nuclei has

led to a constraint of $E_{\mathrm{sym}}(\rho_0) = 30.1$ MeV and $L = 51.5$ MeV, which is shown by solid up-triangle with a label "**Iso. Diff. (2010)**" in Fig. 1.

The isospin effects of fragment transverse flows in heavy ion collisions are useful for extracting information on the symmetry energy. In a recent work,[21] the transverse flow of intermediate mass fragments (IMFs) has been investigated for the 35 MeV/u ^{70}Zn $+^{70}$Zn, ^{64}Zn $+$ ^{64}Zn, and ^{64}Ni $+$ ^{64}Ni systems. The analysis based on the AMD model with the GEMINI code treatment for statistically de-excitation of the hot fragments leads to a constraint $E_{\mathrm{sym}}(\rho_0) = 30.5$ MeV and $L = 65$ MeV, which is shown by solid diamond with a label "**Trans. Flow (2010)**" in Fig. 1.

3.1.2. *Nucleon optical potential*

Experimentally, there have accumulated a lot of data for elastic scattering of proton (and neutron) from different targets at different beam energies and (p,n) charge-exchange reactions between isobaric analog states. These data provide the possibility to extract information on the isospin dependence of the nucleon optical potential, especially the energy dependence of the nuclear symmetry potential. Based on the Hugenholtz-Van Hove theorem, it has been shown recently[22–24] that both $E_{\mathrm{sym}}(\rho_0)$ and L can be completely and analytically determined by the nucleon optical potentials. Averaging all nuclear symmetry potentials constrained by world data available in the literature since 1969 from nucleon-nucleus scatterings, (p,n) charge-exchange reactions, and single-particle energy levels of bound states, the constraint $E_{\mathrm{sym}}(\rho_0) = 31.3 \pm 4.5$ MeV and $L = 52.7 \pm 22.5$ MeV are simultaneously obtained,[22] and this constraint is indicated by the gray band with a label "**Opt. Pot. (2010)**" in Fig. 1.

3.2. *Nuclear structures*

In recent years, more and more constraints on the symmetry energy have been obtained from the analyses of nuclear structure properties, such as the nuclear mass (ground state binding energy), the neutron skin thickness, the nuclear isobaric analog state energies, and pygmy dipole resonances. We summarize these constraints in the following.

3.2.1. *Nuclear mass*

The nuclear mass data are probably the most accurate, richest, and least ambiguous in the nuclear data library. The Thomas-Fermi model analysis[25] of 1654 ground state mass of nuclei with $N, Z \geq 8$ has given rise to

6

$E_{\mathrm{sym}}(\rho_0) = 32.65$ MeV and $L = 49.9$ MeV, which is shown by solid star with a label "**TF+Nucl. Mass (1996)**" in Fig. 1.

The symmetry energy coefficients $a_{\mathrm{sym}}(A)$ of finite nuclei with mass numbers $A = 20-250$ were determined from more than 2000 precisely measured nuclear masse.[26] With the semiempirical connection between $a_{\mathrm{sym}}(A)$ and the symmetry energy at reference densities, i.e., $E_{\mathrm{sym}}(\rho_A) \approx a_{\mathrm{sym}}(A)$, and assuming a symmetry energy with density dependence of $E_{\mathrm{sym}}(\rho) = E_{\mathrm{sym}}(\rho_0)(\rho/\rho_0)^\gamma$, Liu *et al.*[26] obtained a constraint at 95% confidence level shown as a parallelogram with short-dotted-line sides in Fig. 1, labeled "**Nucl. Mass(2010)**".

Within the Skyrme-Hartree-Fock (SHF) approach, it has been shown recently that a value of $E_{\mathrm{sym}}(\rho_A)$ at a subsaturation reference density ρ_A leads to a positive linear correlation between $E_{\mathrm{sym}}(\rho_0)$ and L.[27] Using recently extracted $E_{\mathrm{sym}}(\rho_A = 0.1 \text{ fm}^{-3}) \approx a_{\mathrm{sym}}(A = 208) = 20.22 - 24.74$ MeV at 95% confidence level from more than 2000 measured nuclear masses, Chen[27] obtained a constraint denoted by the region between two thick dash-dotted lines with a label "$E_{\mathbf{sym}}(\rho_A = 0.1 \text{ } \mathbf{fm}^{-3})(\mathbf{2011})$" in Fig. 1.

The finite-range droplet(FRDM) model has been shown to be very successful to describe the nuclear ground state mass. The parameters in the macroscopic droplet part of the FRDM model are related to the properties of the equation of state. Using the new, more accurate FRDM-2011a version, Moller *et al.*[28] analyzed the nuclear mass of the 2003 Atomic Mass Evaluation (AME2003), and obtained the constraint $E_{\mathrm{sym}}(\rho_0) = 32.5 \pm 0.5$ MeV and $L = 70 \pm 15$ MeV shown as a square box bounded by short-dash-dotted lines in Fig. 1, labeled "**FRDM (2012)**".

In a more recent work,[29] Lattimer and Lim used the confidence ellipse method for nuclear mass fitting. Based on a SHF energy-density functional for nuclear masses, they obtained a 95% confidence ellipse for the $E_{\mathrm{sym}}(\rho_0)$-L constraints shown by the thick dashed lines in Fig. 1, labeled "**Nucl. Mass(2012)**".

3.2.2. *Neutron skin thickness*

Theoretically, it has been established[16,30] that the neutron skin thickness of heavy nuclei, given by the difference of their neutron and proton root-mean-squared radii, provides a good probe of $E_{\mathrm{sym}}(\rho)$. The droplet model analyses[31] on the neutron skin sizes measured in 26 antiprotonic atoms along the mass table leads to the constraint $E_{\mathrm{sym}}(\rho_0) = 28 - 35$ MeV and $L = 30 - 80$ MeV shown as a square box bounded by dash-dotted lines in

Fig. 1, labeled "**DM+N-Skin (2009)**".

A microscopic SHF analysis[32] on the neutron skin thickness of Sn isotopes has led to a set of constraints corresponding to 95% confidence levels, shown as a region bounded by two short-dashed curves in Fig. 1, labeled "**SHF+N-Skin (2010)**".

3.2.3. *Nuclear isobaric analog state energies*

The nuclear isobaric analog state (IAS) energies are believed to provide a particularly clean and useful probe of the symmetry energy since the ambiguities in the determination of the symmetry energy of finite nuclei from binding energies caused by the Coulomb term can be removed.[33] By fitting the available data on the IAS and using the droplet surface symmetry energy, Danielewicz and Lee[34] obtained the constraint shown as a parallelogram bounded by dashed lines in Fig. 1, labeled "**IAS+LDM (2009)**".

3.2.4. *Pygmy dipole resonance*

The experimentally observed pygmy dipole (E1) strength might play an equivalent role as the neutron rms radius in constraining the symmetry energy.[35] Excess neutrons forming the skin give rise to pygmy dipole transitions at excitation energies below the giant dipole resonance, and such transitions could represent a collective vibration of excess neutrons against an isospin symmetric core. Comparing the measured pygmy dipole strength in ^{130,132}Sn to that obtained within a relativistic mean-field approach, Klimkiewicz *et al.*[36] obtained the constraint $E_{sym}(\rho_0) = 30.2 - 33.8$ MeV and $L = 28.1 - 58.1$ MeV shown as a square box bounded by think solid lines in Fig. 1, labeled "**PDR (2007)**". Another analysis[37] on the measured pygmy dipole strength in ^{68}Ni and ^{132}Sn within the relativistic and non-relativistic mean-field approaches leads to the constraint $E_{sym}(\rho_0) = 31.0 - 33.6$ MeV and $L = 49.1 - 80.5$ MeV shown as a square box bounded by dash-dot-dotted lines in Fig. 1, labeled "**PDR (2010)**".

3.3. *The properties of neutron stars*

Astrophysical observations of neutron star masses and radii provide important probe for the equation of state of neutron-rich matter. In particular, neutron star radii are strongly correlated with neutron matter pressures around the saturation density.[38]

In a recent work,[39] Steiner and Gandolfi demonstrated that currently

available neutron star mass and radius measurements provide a significant constraint on the EOS of neutron matter. Using a phenomenological parametrization for EOS of neutron matter near and above the saturation density with partial parameters determined by the quantum Monte Carlo calculations, they obtained a constraint of $E_{\mathrm{sym}}(\rho_0) = 31.2 - 34.3$ MeV and $L = 36 - 55$ MeV at 95% confidence level based on Bayesian analysis,[39,40] and this constraint is shown as a square box bounded by thick solid lines in Fig. 1, labeled "**NStar1 (2012)**". More recently, Lattimer and Lim[29] performed a similar Bayesian analysis of the available neutron star mass and radius measurements, they obtained a constraint of $E_{\mathrm{sym}}(\rho_0) = 28 - 34$ MeV and $L = 40 - 60$ MeV shown as a square box bounded by thick short-dahsed lines in Fig. 1, labeled "**NStar2 (2012)**".

Besides neutron star mass and radius, other properties of neutron stars may also put constraints on the symmetry energy. For example, the binding energy of neutron stars,[41] the frequencies of torsional crustal vibrations[42,43] and the r-model instability window[44] all consistently favor L values less than about 70 MeV.

3.4. *Discussions*

In Fig. 1, we include totally 18 constraints on L and $E_{\mathrm{sym}}(\rho_0)$ described above. Obviously, it cannot be that all the constraints are equivalently reliable since some constraints do not have overlap. It should be stressed that the symmetry energy cannot be measured directly and each constraint shown in Fig. 1 is based on a certain theoretical model with some approximations or special assumptions.

We would like to highlight two constraints in Fig. 1, i.e., "**SHF+N-Skin (2010)**" and "$E_{\mathbf{sym}}(\rho_A = 0.1\ \mathbf{fm}^{-3})(\mathbf{2011})$" since both constraints are based on the same SHF analysis with 95% confidence. The two constraints are re-plotted in Fig. 2. It is very interesting to see that while the constraint "$E_{\mathbf{sym}}(\rho_A = 0.1\ \mathbf{fm}^{-3})(\mathbf{2011})$" indicates a linear positive correlation between L and $E_{\mathrm{sym}}(\rho_0)$, the constraint "**SHF+N-Skin (2010)**" displays a negative correlation. Actually, only the constraint "**SHF+N-Skin (2010)**" among the 18 constraints displays such negative correlation. This interesting feature makes the constraint "**SHF+N-Skin (2010)**" particularly important as combing it with other constraints will significantly improve the constraint on L and $E_{\mathrm{sym}}(\rho_0)$. It is interesting to see that the overlap of "**SHF+N-Skin (2010)**" and "$E_{\mathbf{sym}}(\rho_A = 0.1\ \mathbf{fm}^{-3})(\mathbf{2011})$" is consistent with all the other constraints shown in Fig. 1 except "**IAS+LDM (2009)**". The latter neglected the higher-order density curvature contribu-
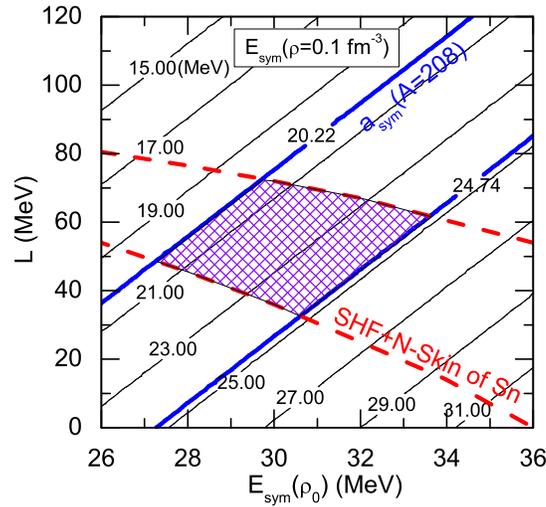
Fig. 2.   (Color online) Contour curves in the $E_{\mathrm{sym}}(\rho_0)$ -L plane for $E_{\mathrm{sym}}(\rho = 0.1$ $\mathrm{fm}^{-3})$ from SHF calculations. The region between the two thick solid lines represents the constraint obtained with 20.22 MeV $\leq E_{\mathrm{sym}}(\rho_A = 0.10\ \ \mathrm{fm}^{-3})$ $\leq$24.74 MeV while the region between the two thick dashed lines is the constraint from the SHF analysis of neutron skin data of Sn isotopes within a 2σ uncertainty.[32] The shaded region represents the overlap of the two constraints. Taken from Ref.[27]

tion of the symmetry energy and its inclusion may reduce the L value[29] (See also Ref.[27]).

The positive correlation between L and $E_{\mathrm{sym}}(\rho_0)$ from "$E_{\mathbf{sym}}(\rho_A = 0.1$ $\mathbf{fm}^{-3})(\mathbf{2011})$" has been clearly demonstrated in Ref.,[27] This feature implies that nuclear mass fitting should lead to positive correlation between L and $E_{\mathrm{sym}}(\rho_0)$ since $E_{\mathrm{sym}}(\rho_A = 0.1\ \mathrm{fm}^{-3})$ reflects the symmetry energy of finite nuclei, which is demonstrated by the nice agreement between the constraints "$E_{\mathbf{sym}}(\rho_A = 0.1\ \mathbf{fm}^{-3})(\mathbf{2011})$" and "$\mathbf{Nucl.\ Mass(2012)}$".

The negative correlation between L and $E_{\mathrm{sym}}(\rho_0)$ from "$\mathbf{SHF+N\text{-}Skin}$ $(\mathbf{2010})$" can be understood from the fact that the neutron skin thickness is determined by the neutron and proton pressure difference at sub-saturation density, namely, the density slope of symmetry energy at sub-saturation density (rather than L), which increases with both L and $E_{\mathrm{sym}}(\rho_0)$.[45]

From Fig. 1 and Fig. 2, we can see that while $E_{\mathrm{sym}}(\rho_0)$ and L can vary largely depending on the data or methods, all the constraints are essentially consistent with $E_{\mathrm{sym}}(\rho_0) = 31 \pm 2$ MeV and $L = 50 \pm 20$ MeV.

10

4. The symmetry energy at supra-saturation densities

While significant progress has been made on constraining the symmetry energy around the saturation density, the supra-saturation density behavior of the symmetry energy remains elusive and largely controversial. FOPI data on the π^-/π^+ ratio in central heavy-ion collisions at SIS/GSI energies favor a quite soft symmetry energy at $\rho \geq 2\rho_0$ from the isospin and momentum dependent IBUU04 model analysis[9] while an opposite conclusion has been obtained from the improved isospin dependent quantum molecular dynamics (ImIQMD) model analysis.[10] It should be mentioned that the ImIQMD model analysis did not consider the energy dependent symmetry potential and it cannot explain qualitatively the isospin fractionation phenomenon observed in heavy ion collisions.[46,47] A further careful check is definitely needed to understand the model dependence.

In a more recent work, Russotto *et al.*[11] analyzed the elliptic-flow ratio of neutrons with respect to protons or light complex particles from the existing FOPI/LAND data for $^{197}\text{Au} + {}^{197}\text{Au}$ collisions at 400 MeV/nucleon within the UrQMD model, and they obtained a moderately soft symmetry energy with a density dependence of the potential term proportional to $(\rho/\rho_0)^\gamma$ with $\gamma = 0.9 \pm 0.4$.

Besides using heavy ion collisions to constrain the supra-saturation density behavior of the symmetry energy, it has been proposed recently[48] that the three bulk characteristic parameters $E_{\text{sym}}(\rho_0)$, L and K_{sym} essentially determine the symmetry energy with the density up to about $2\rho_0$. This opens a new window to constrain the supra-saturation density behavior of the symmetry energy from its density behaviors at the saturation density.

5. Summary

Significant progress has been made both experimentally and theoretically on constraining the density dependence of the symmetry energy after more than one decade of studies in the community. Although the values of $E_{\text{sym}}(\rho_0)$ and L can vary largely depending on the data or methods, all the constraints obtained so far from nuclear reactions, nuclear structures, and the properties of neutron stars are essentially consistent with $E_{\text{sym}}(\rho_0) = 31 \pm 2$ MeV and $L = 50 \pm 20$ MeV. More high quality data and more accurate theoretical methods are needed to further reduce the theoretical and experimental uncertainties of the constraints on $E_{\text{sym}}(\rho)$ around the saturation density. In contrast, the determination of the supra-saturation density behavior of the symmetry energy is still largely controversial and

remains a big challenge in the community.

Acknowledgments

References

1. J.M. Lattimer and M. Prakash, *Science* **304**, 536 (2004); *Phys. Rep.* **442**, 109 (2007).
2. A.W. Steiner *et al.*, *Phys. Rep.* **411**, 325 (2005).
3. V. Baran, M.Colonna, V. Greco, and M. Di Toro, *Phys. Rep.* **410**, 335 (2005).
4. L.W. Chen, C.M. Ko, B.A. Li, and G.C. Yong, Front. Phys. China **2**, 327 (2007) [arXiv:0704.2340].
5. B.A. Li, L.W. Chen, and C.M. Ko, *Phys. Rep.* **464**, 113 (2008).
6. C.J. Horowitz, S.J. Pollock, P.A. Souder, and R. Michaels, *Phys. Rev.* **C63**, 025501 (2001).
7. T. Sil, M. Centelles, X. Viñas, and J. Piekarewicz, *Phys. Rev.* **C71**, 045502 (2005).
8. D.H. Wen, B.A. Li, and L.W. Chen, *Phys. Rev. Lett.* **103**, 211102 (2009).
9. Z.G. Xiao, B.A. Li, L.W. Chen, G.C. Yong, and M. Zhang, *Phys. Rev. Lett.* **102**, 062502 (2009).
10. Z.Q. Feng and G.M. Jin, *Phys. Lett.* **B683**, 140 (2010).
11. P. Russotto, P.Z. Wu, M. Zoric, M. Chartier, Y. Leifels, R.C. Lemmon, Q. Li, J. Lukasik, A. Pagano, P. Pawlowski, and W. Trautmann, *Phys. Lett.* **B697**, 471 (2011).
12. C. Xu and B.A. Li, *Phys. Rev.* **C81**, 064612 (2010).
13. B.J. Cai and L.W. Chen, *Phys. Rev.* **C85**, 024302 (2012).
14. L.W. Chen, C.M. Ko, and B.A. Li, *Phys. Rev. Lett.* **94**, 032701 (2005); B.A. Li and L.W. Chen, *Phys. Rev.* **C72**, 064611 (2005).
15. M. B. Tsang et al., *Phys. Rev. Lett.* **92**, 062701 (2004).
16. L.W. Chen, C.M. Ko, and B.A. Li, *Phys. Rev.* **C72**, 064309(2005).

12

17. M. B. Tsang et al., *Phys. Rev. Lett.* **86**, 5023 (2001).
18. D. Shetty, S.J. Yennello, and G.A. Souliotis, *Phys. Rev.* **C75**, 034602 (2007).
19. M.B. Tsang *et al.*, *Phys. Rev. Lett.* **102**, 122701 (2009).
20. Z.Y. Sun *et al.*, *Phys. Rev.* **C82**, 051603(R) (2010).
21. Z. Kohley *et al.*, *Phys. Rev.* **C82**, 064601 (2010).
22. C. Xu, B.A. Li, and L.W. Chen, *Phys. Rev.* **C82**, 054607 (2010).
23. C. Xu, B.A. Li, L.W. Chen, and C.M. Ko, *Nucl. Phys.* **A865**, 1 (2011).
24. R. Chen, B.J. Cai, L.W. Chen, B.A. Li, X.H. Li, and C. Xu, *Phys. Rev.* **C85**, 024305 (2012).
25. W.D. Myers and W.J. Swiatecki, *Nucl. Phys.* **A601**, 141 (1996).
26. M. Liu, N. Wang, Z.X. Li, and F.S. Zhang, *Phys. Rev.* **C82**, 064306 (2010).
27. L.W. Chen, *Phys. Rev.* **C83**, 044308 (2011).
28. P. Moller, W.D. Myers, H. Sagawa, and S.Yoshida, *Phys. Rev. Lett.* **108**, 052501 (2012)
29. J.M. Lattimer and Y. Lim, arXiv:1203.4286.
30. B.A. Brown, *Phys. Rev. Lett.* **85**, 5296 (2000); S. Typel and B.A. Brown, *Phys. Rev.* **C64**, 027302 (2001).
31. M. Centelles *et al.*, *Phys. Rev. Lett.* **102**, 122502 (2009); M. Warda *et al.*, *Phys. Rev.* **C80**, 024316 (2009).
32. L.W. Chen, C.M. Ko, B.A. Li, and J. Xu, *Phys. Rev.* **C82**, 024321 (2010).
33. P. Danielewicz, *Nucl. Phys.* **A727**, 233 (2003).
34. P. Danielewicz and J. Lee, *Nucl. Phys.* **A818**, 36 (2009).
35. J. Piekarewicz, *Phys. Rev.* **C73**, 044325 (2006).
36. A. Klimkiewicz *et al.*, *Phys. Rev.* **C76**, 051603(R) (2007).
37. A. Carbone, G. Colò, A. Bracco, L.G. Cao, P.F. Bortignon, F. Camera, and O. Wieland, *Phys. Rev.* **C81**, 041301 (R) (2010).
38. J. M. Lattimer and M. Prakash, *Astrophys. J.* **550**, 426 (2001).
39. A. W. Steiner and S. Gandolfi, *Phys. Rev. Lett.* **108**, 081102 (2012).
40. M.B. Tsang *et al.*, arXiv:1204.0466.
41. W. Newton and B.A. Li, *Phys. Rev.* **C80**, 065809 (2009).
42. A.W. Steiner and A.L. Watts, *Phys. Rev. Lett.* **103**, 181101 (2009).
43. M. Gearheart, W.G. Newton, J. Hooker, and B.A. Li, *MNRAS* **418**, 2343 (2011).
44. D.H. Wen, W.G. Newton, and B.A. Li, *Phys. Rev.* **C85**, 025801 (2012).
45. L.W. Chen, unpublished, 2012.
46. H.S. Xu *et al.*, *Phys. Rev. Lett.* **85**, 716 (2000).
47. B.A. Li, *Phys. Rev. Lett.* **88**, 192701 (2002).
48. L.W. Chen, *Science China: Physics, Mechanics and Astronomy* **54**, s124 (2011) [arXiv:1101.2384].